CIVIL ENGINEERING JOURNAL

Article no. 28

THE CIVIL ENGINEERING JOURNAL 3-2024

DYNAMIC PERFORMANCE ANALYSIS OF CABLE DAMAGE IN PRESTRESSED Π-SHAPED BEAM CABLE-STAYED BRIDGE

Xilong Zheng[1] and Honglei Zhang[2]

1. *School of Civil and Architectural Engineering, Harbin University, No.109 Zhongxing Road, Harbin, Heilongjiang Province, China; sampson88@126.com*
2. *Bridge Department, Beijing New Bridge Technology Development Co., LTD, No.8 Xitucheng Road, Beijing, China*

ABSTRACT

This paper takes a prestressed π-shaped beam cable-stayed bridge in China as an engineering case, and conducts relevant research on the overall and local parameter sensitivity of the structure and the stress characteristics under cable damage. The main factors causing cable damage in the prestressed π-shaped beam cable-stayed bridge are analyzed, and the selection of elastic modulus as a damage variable is determined. Based on the finite element model analysis of the actual bridge, different inclined cables are selected for damage simulation, and the dynamic variation characteristics of the main beam, cables, and other structures under one-sided, symmetrical, and asymmetrical cable damage are analyzed. This provides a reference for the dynamic performance analysis of prestressed π-shaped beam cable-stayed bridges under similar cable damage conditions in the future.

KEYWORDS

Cable-stayed bridge, π-shaped beam, Finite element analysis, Static performance

INTRODUCTION

Currently, in the design of cable-stayed bridges, the maximum span exceeds 400m, and the main beam form is mainly steel or composite beams, while for spans below 400m, the preferred main beam forms are prestressed concrete box girders or π-shaped beams [1-3]. The development of cable-stayed bridges has become increasingly mature, but it also brings more and more challenging problems. Currently, the detection and maintenance of cable-stayed bridges are not yet in a mature stage. As the lifeline of cable-stayed bridges, the cable plays a crucial role and is also the most susceptible to damage. Therefore, scholars at home and abroad have conducted in-depth research on this important structure [4,5].

Not only do structural parameters have a significant impact on the stress performance of cable-stayed bridges, but also certain external accidental factors during operation can lead to changes in their stress performance [6-8]. As the lifeline of cable-stayed bridges, the cables are generally in good operational condition, but a few cable-stayed bridges have experienced varying degrees of issues. Due to the existence of cables, the main beam belongs to a multiple point elastic support system, and its stress characteristics are similar to those of a multi-span continuous beam bridge, which significantly reduces the bending moment of the main beam. The cables, as critical components of the whole system, bear most of the load acting on the main beam [9-12]. However, in daily operation, factors such as damaged sheathing, wire corrosion, and vibration fatigue can

cause varying degrees of damage to the cables. Cable damage leads to a redistribution of cable forces across the entire bridge and can result in varying degrees of deflection changes in the main beam, directly influencing the bridge's service life. Currently, the research on cable damage is mainly focused on integral box girder cable-stayed bridges, and there is relatively less research on the impact of cable damage on π-shaped beam cable-stayed bridges [13,14].

There is still no definitive standard for the causes of cable damage, the impact on cable-stayed bridge performance, and how to accurately determine the location and degree of cable damage. Cable damage is inevitable during normal operation due to various reasons. How to make accurate assessments of cable damage and develop effective testing methods is a difficult problem that cable-stayed bridges face [15]. In this article, a prestressed π-shaped beam cable-stayed bridge engineering example is used to identify the impact of parameter changes and cable damage on the stress performance of the bridge. By changing the elastic modulus of the cables to simulate cable damage, the trend of changes in cable tension, main beam vertical displacement, and overall structural frequency under various cable damage conditions were analyzed, and the influence of cable damage on the structural mechanics performance of the prestressed π-shaped beam cable-stayed bridge was obtained.

INTRODUCTION TO ENGINEERING BACKGROUND

The engineering background of this article is a prestressed π-shaped beam single-tower cable-stayed bridge in Jilin Province. The total length of the prestressed π-shaped beam cable-stayed bridge is 617.06 m, with a span combination of (4×30) m + (39.9+89.1+151) m + (4×30) m + (3×30) m, and the main bridge section for study is the second section. The main bridge adopts an "H" shaped single-tower double-cable-plane PC beam cable-stayed bridge, with a span combination of 39.9 m + 89.1 m + 151 m. The main bridge structure is a fixed system, with a 2.0% bi-directional transverse slope and a design load of Class-A city. There are a total of 18 pairs of spatial cables arranged in a fan shape on the main tower. The cables are arranged on the main beam cross-section at a distance of 0.8m from the edge of the main beam. The layout of the prestressed π-shaped beam cable-stayed bridge is shown in Figure 1. Cross section diagram of the main bridge is shown in Figure 2.

1. Main beam structure

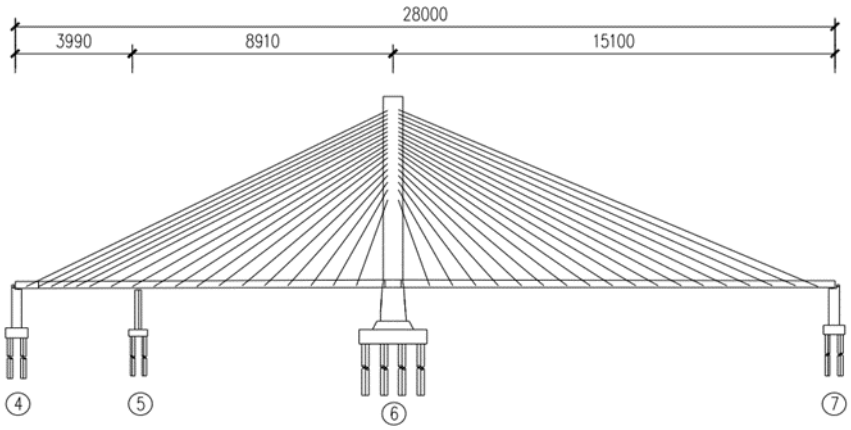

Fig. 1 – Layout diagram of the main bridge (unite: cm)

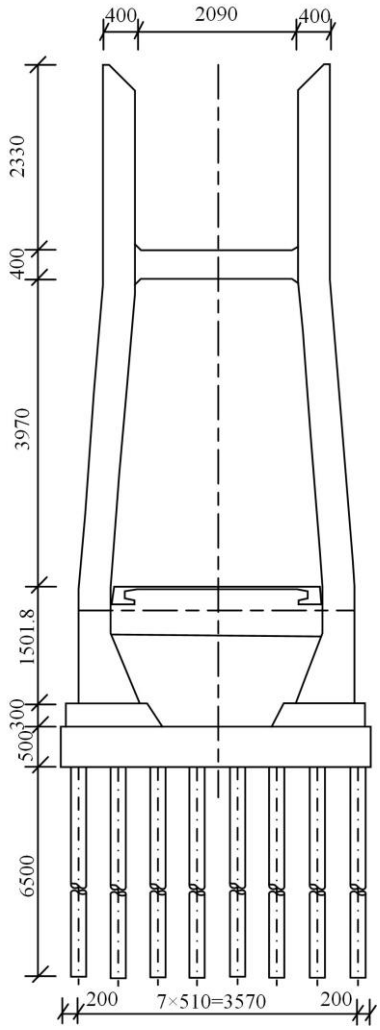

Fig. 2 – Cross section diagram of the main bridge (unite: cm)

The main beam adopts a pre-stressed concrete "π" shaped cross-section. The width of the main beam section is 26.5 m, and the height is 2.3 m. It is designed with a bidirectional 2% cross slope. The basic spacing of the transverse beams is 3.9 m, 3.65 m, and 4.25 m. The transverse beams are all equipped with pre-stressed steel hinge lines. The main beam is connected to the main tower using a fixed system, and both the main beam and the transverse beams are made of C55 concrete.

2. Main tower

The main tower of the cable-stayed bridge adopts an H-shaped main tower. The height of the main tower is 117.318 m. The cross-section of the tower column is a hollow rectangular shape, with a full width of 6.8 m in the middle and upper tower columns longitudinally, and a width of 4.0 m in the transverse bridge direction. The upper part of the lower tower column gradually increases from a width of 6.8 m to a full width of 8.8 m longitudinally, and the width in the transverse bridge direction gradually increases to 7.5 m.

The cross-section of the transverse beam is a hollow rectangular shape. The upper transverse beam has a rectangular cross-section of 6.2 m × 4 m, while the lower transverse beam has a width of 6.4 m and a height ranging from 6 m to 6.27 m. A tower pedestal with a height of 3 m is provided at the top of the main tower's bearing platform. Except for the lower transverse beam, which is made

of C55 concrete, the rest of the main tower structures are made of C50 concrete.

3. Stay cable

The main tower is equipped with a total of 72 stay cables, with each cable spaced at a designed interval of 7.8 m. The cable spacing changes to 7.8 m, 7.3 m, and 4.25 m corresponding to the length variations of the main span's cast-in-place segments. The stay cables are positioned 0.8 m away from the edge of the main beam cross-section. The stay cables are all made of Φs 15.2 steel strand with a standard strength of 1860 MPa. The stay cable numbering is shown in Figure 3.

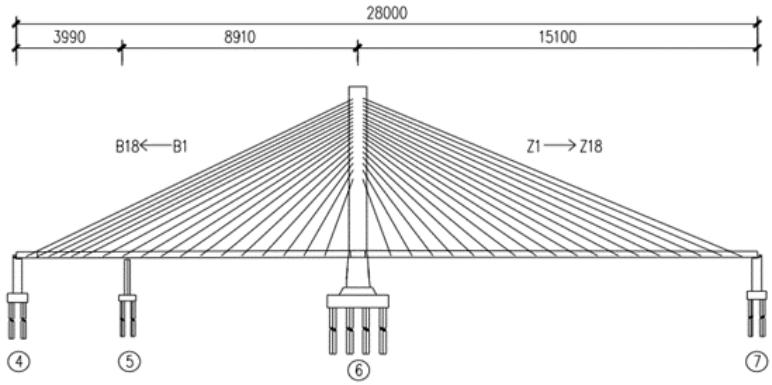

Fig. 3 – Stay cable numbering diagram

FINITE ELEMENT ANALYSIS MODEL

The finite element model of this prestressed π-type girder cable-stayed bridge is established and analyzed using the specialized bridge analysis software, Midas Civil. The main beam and main tower are simulated using 2D beam elements, with section dimensions set to match the actual conditions. The overall finite element model of the prestressed π-type girder cable-stayed bridge consists of 483 nodes and 399 elements, with 327 beam elements, including 235 main beam elements and 92 main tower elements. There are 72 truss (stay cable) elements that only experience tension. The complete bridge finite element model is shown in Figure 4.

The main beam and main tower are simulated in the cable-stayed bridge using the shared node approach to model the fixed support system. The auxiliary piers and main beam are rigidly connected, and the connection between the stay cable anchorage points, main beam, and main tower is simulated using rigid connections as well. The transverse beams on the main beam and main tower are made of C55 concrete. The lower transverse beam of the main tower, upper tower columns, middle tower columns, lower tower columns, and tower base are made of C50 concrete. The 5# auxiliary pier is made of C40 concrete.

Both longitudinal and transverse prestressing tendons are made of high-strength low-relaxation prestressing strand with a single strand diameter of Φs 15.2 mm. The standard strength of the strand is 1860 MPa, with an elastic modulus of 1.95×10^5 MPa, and a cross-sectional area of 140 mm^2.

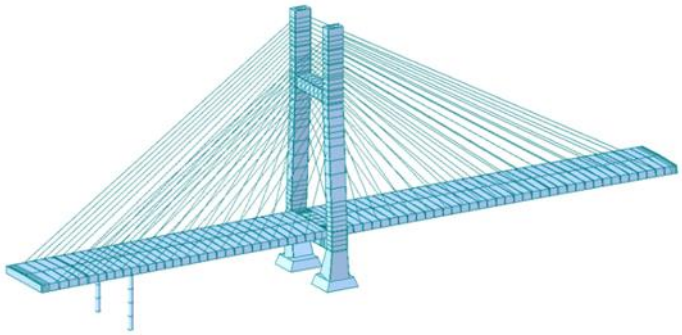

Fig. 4 – The finite element model of the main bridge

DYNAMIC PERFORMANCE ANALYSIS OF PRESTRESSED Π-TYPE BEAM CABLE-STAYED BRIDGE UNDER SIMILAR CABLE DAMAGE CONDITIONS

In this section, the first 10 vibration modes of the prestressed π-type beam cable-stayed bridge model were obtained through the finite element software Midas Civil. By modifying the elastic modulus of the cable, simulations were conducted on the cable damage location and degree under different working conditions, and the changes in dynamic characteristics of the prestressed π-type beam cable-stayed bridge were studied. As a result, the relationship between cable damage location and degree and changes in dynamic characteristics was derived. The first 10 vibration modes of the cable in undamaged condition are shown in Figure 5 - Figure 14, with frequencies and periods listed in Table 1.

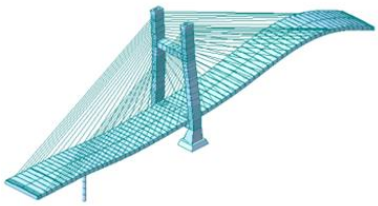

Fig. 5 – The first-order array diagram

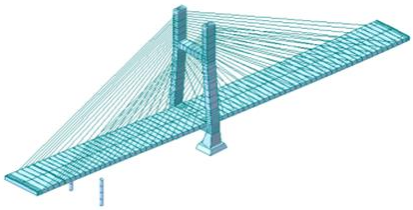

Fig. 6 – The second-order array diagram

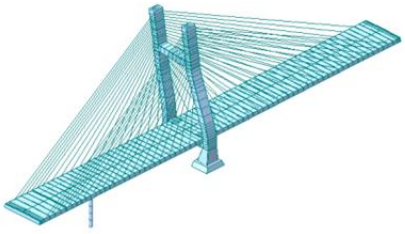

Fig. 7 – The third-order array diagram

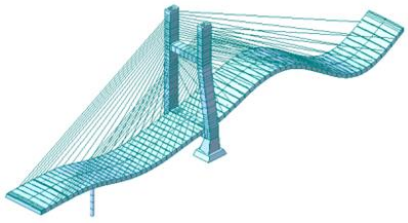

Fig. 8 – The fourth-order array diagram

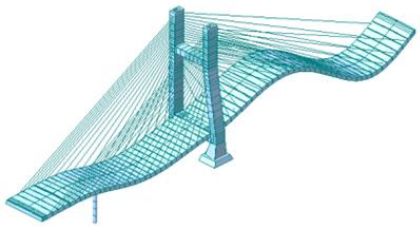

Fig. 9 – The fifth-order array diagram

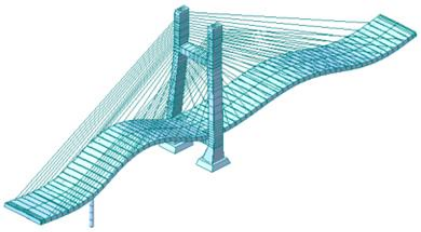

Fig. 10 – The sixth-order array diagram

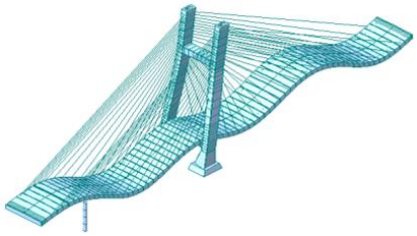

Fig. 11 – The seventh-order array diagram

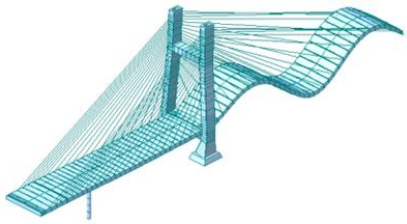

Fig. 12 – The eighth-order array diagram

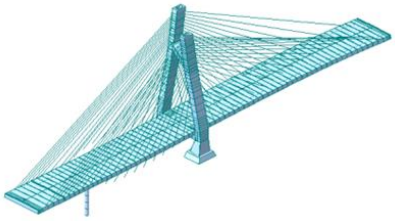

Fig. 13 – The ninth-order array diagram

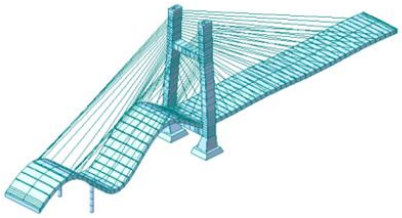

Fig. 14 – The tenth-order array diagram

Tab. 1 - Dynamics characteristics table of a prestressed π-Type beam cable-stayed bridge

Order	Frequency (Hz)	Period (s)	Description of the waveform
1	0.643	1.556	Main tower right side main girder first-order vertical bending
2	0.988	1.012	Main girder lateral deflection
3	1.139	0.876	Tower column lateral bending
4	1.271	0.787	Main tower right side main girder second-order vertical bending
5	1.298	0.770	Main girder vertical oscillation
6	1.428	0.700	Main tower both sides main girder first-order symmetric vertical bending
7	1.839	0.544	Main tower both sides main girder second-order symmetric vertical bending
8	2.131	0.469	Main tower right side main girder third-order vertical bending
9	2.401	0.416	Tower column lateral symmetric bending
10	2.727	0.367	Main tower left side main girder third-order vertical bending

Dynamic Performance Analysis of Single-Side Cable-Stayed Bridge with Similar Damage Level

For the analysis of different cable-stayed bridges with varying damage levels of 60% on auxiliary spans and short main spans, eight scenarios are selected: B1, B3, B6, B8, B10, B12, B16, and B18. The definition of each scenario is provided in Table 2.

Tab. 2 - Table of Natural Frequencies and Mode Shapes of Structures with Different Cable Damage Levels on Auxiliary Spans and Short Main Spans

Order	Non-destructive	B1 60%	B3 60%	B6 60%	B8 60%	B10 60%	B12 60%	B16 60%	B18 60%	Theoretical model mode of vibration
1	0.642	0.642	0.642	0.642	0.641	0.639	0.638	0.636	0.636	First-order vertical bending of the main beam on the right side of the main tower
2	0.987	0.987	0.987	0.987	0.987	0.987	0.987	0.987	0.987	Lateral deflection of the main beam
3	1.138	1.136	1.136	1.136	1.136	1.136	1.136	1.136	1.136	Lateral bending of the tower column
4	1.270	1.269	1.266	1.266	1.269	1.269	1.268	1.268	1.268	Second-order vertical bending of the main beam on the right side of the main tower
5	1.298	1.297	1.297	1.297	1.297	1.297	1.297	1.297	1.297	Vertical deflection of the main beam
6	1.42	1.423	1.406	1.398	1.418	1.427	1.425	1.424	1.425	First-order symmetrical vertical bending of the main beam on both sides of the main tower
7	1.83	1.830	1.826	1.817	1.821	1.82	1.828	1.828	1.827	Second-order symmetrical vertical bending of the main beam on both sides of the main tower
8	2.130	2.129	2.129	2.129	2.129	2.129	2.129	2.129	2.129	Third-order vertical bending of the main beam on the right side of the main tower
9	2.401	2.399	2.399	2.399	2.396	2.383	2.377	2.371	2.367	Symmetrical lateral bending of the tower column
10	2.726	2.713	2.699	2.725	2.714	2.721	2.726	2.725	2.726	Third-order vertical bending of the main beam on the left side of the main tower

Due to the difficulty of directly observing the frequency variations in each damaged scenario, calculating the frequency variations for each scenario can provide a more intuitive understanding of the frequency and mode shape changes. To facilitate a more direct comparison of the frequency variations on the cable-stayed bridge's auxiliary spans and short main spans in different damaged scenarios, the eight scenarios mentioned above are compared separately based on cable position.

Please refer to Figure 15 - Figure 18 for the graphical representation of these comparisons.

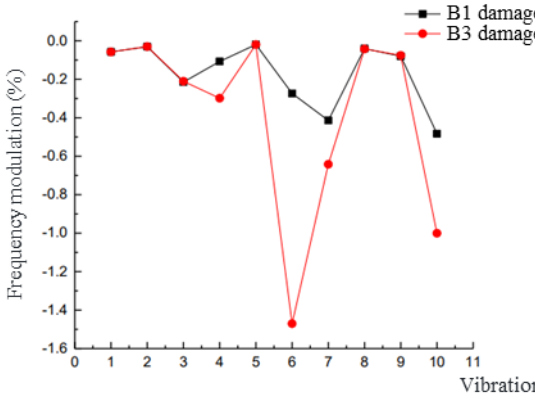

Fig. 15 – The location of the auxiliary span and the inner side of the short main span

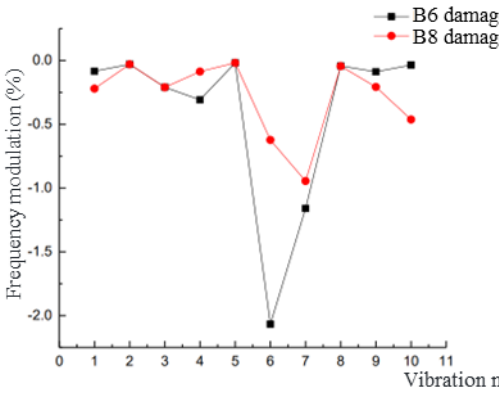

Fig. 16 – The position of 1/3L to 1/2L of the auxiliary span and the short main span

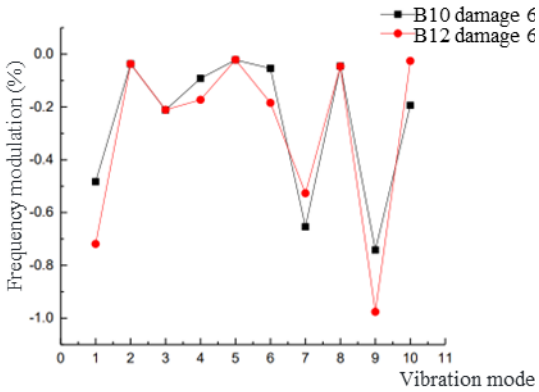

Fig. 17 – The position of 1/2 to 2/3L of the auxiliary span and the short main span

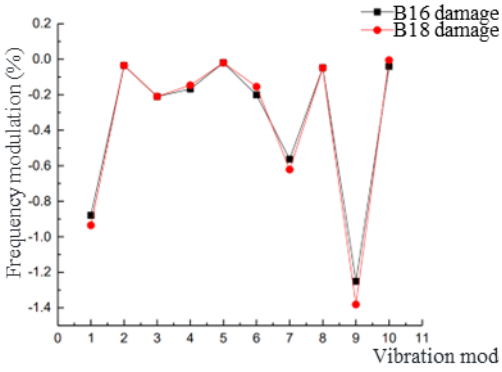

Fig. 18 – The outermost position of the auxiliary span and the short main span

Damage to the diagonal cables of the auxiliary span and short main span has almost no effect on the lateral or vertical deflection of the main beam or the high-order vertical bending of the right main beam of the main tower. Damage to the diagonal cables within 1/2 L near the auxiliary span and short main span will have a relatively large impact on the sixth-order natural frequency of the structure, with a maximum value of 2.06%. At the same time, it can be observed that the influence of diagonal cable damage on the sixth-order natural frequency within the auxiliary span and short main span increases with distance from the main tower, but the trend is opposite within the range of 1/3 L~1/2 L.

Damage to the diagonal cables within the range of 1/2 L near the auxiliary span and short main span shows a consistent trend, all of which have a significant impact on the ninth-order natural frequency. The further the damaged diagonal cables are from the main tower, the greater the impact on the ninth-order natural frequency.

To compare the frequency variations under different levels of 60% damage to the diagonal cables of the long main span, eight different scenarios (Z1, Z3, Z6, Z8, Z10, Z12, Z16, Z18) were selected for analysis. The definition of each scenario can be found in Table. 4 - Table. 10.

In order to visually compare the frequency changes under different damage conditions, the eight scenarios are compared separately according to the position of the diagonal cables, as shown in

Figure19 - Figure 22.

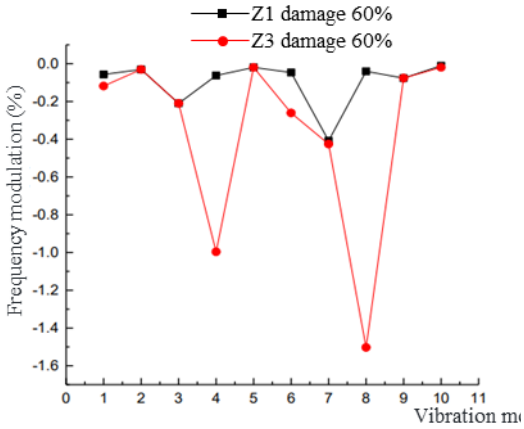

Fig. 19 – The inner side of the long main span

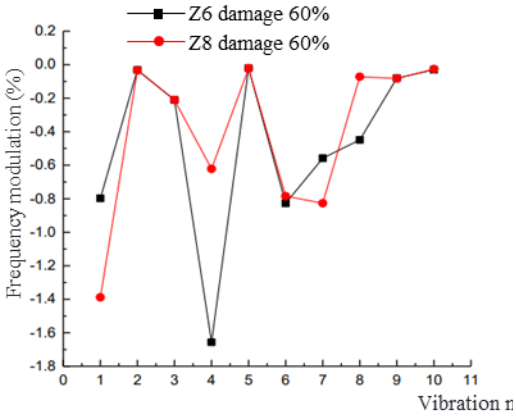

Fig. 20 – The position of 1/3L to 1/2L of the long main span

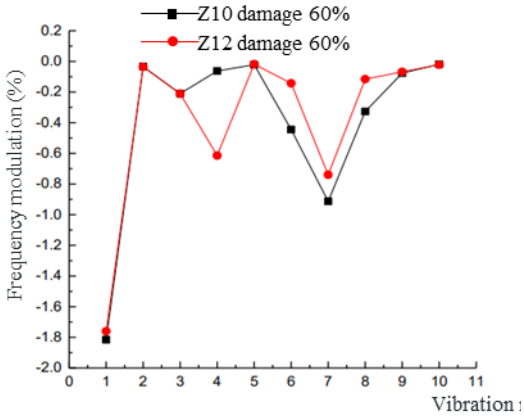

Fig. 21 – The position of 1/2 to 2/3L of the long main span

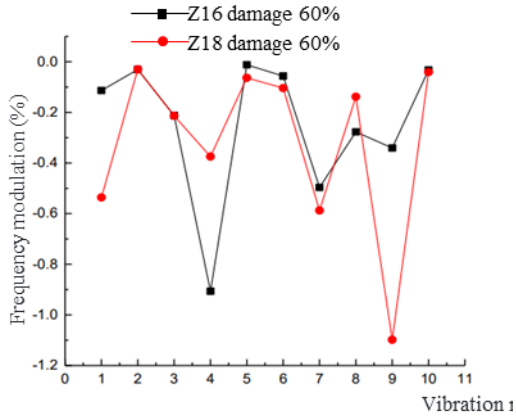

Fig. 22 – The outer side position of the long main span

Damage to the inclined cables at the outer position of the long main span has almost no impact on the lateral and vertical deflection of the main beam and the higher-order vertical bending of the main tower's left side. The damage to the innermost Z1 inclined cable has a minimal effect on the dynamic characteristics of the cable-stayed bridge, with the greatest impact observed on the 7th mode frequency, which is only 0.41%.

Within the range of 1/2 to 2/3L of the long main span, the trend of damage to the inclined cables remains consistent. It has a similar impact on the first mode frequency of the structure, with a maximum frequency variation of 1.82%. However, as the damaged inclined cables are farther from the main tower, they have a greater influence on the 4th mode frequency. The farther the damaged inclined cables are from the tower, the more pronounced the lateral symmetric bending of the tower columns becomes, with a maximum frequency variation of 1.1%.

Analysis of Dynamic Performance under the Same Level of Damage in Symmetric Stay Cables

For the level of damage being equal to 60% in symmetrically positioned cables on both sides of

the main tower, four scenarios, namely B3+Z3, B6+Z6, B12+Z12, and B18+Z18, were selected for analysis, with each scenario described in Table 3.

Tab. 3 - Table of dynamic characteristics for a prestressed π-type girder cable-stayed bridge

Order	Non-destructive	B3+Z3 60%	B6+Z6 60%	B12+Z12 60%	B18+Z18 60%
1	0.643	0.643	0.642	0.637	0.627
2	0.988	0.988	0.987	0.987	0.987
3	1.139	1.139	1.136	1.136	1.136
4	1.271	1.271	1.256	1.248	1.261
5	1.298	1.298	1.298	1.298	1.298
6	1.428	1.428	1.403	1.387	1.424
7	1.839	1.839	1.826	1.814	1.823
8	2.131	2.131	2.099	2.121	2.128
9	2.401	2.401	2.399	2.399	2.378
10	2.727	2.727	2.699	2.725	2.726

The frequencies of the first 10 mode shapes for the aforementioned four damage scenarios are shown in Figure 23. The frequency variations of the first 10 modes for all scenarios are depicted in Figure 24. It can be observed from Figure 23 that after the symmetric stay cables are damaged, the variation in frequencies for each mode shape is very small, with the maximum frequency change amplitude being only 2.89%.

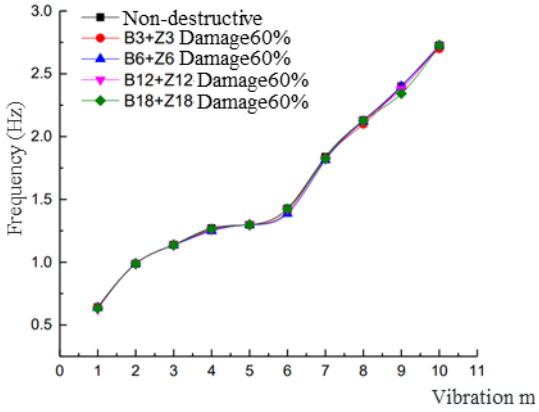

Fig. 23 – The frequency variation graph of symmetrical cable damage

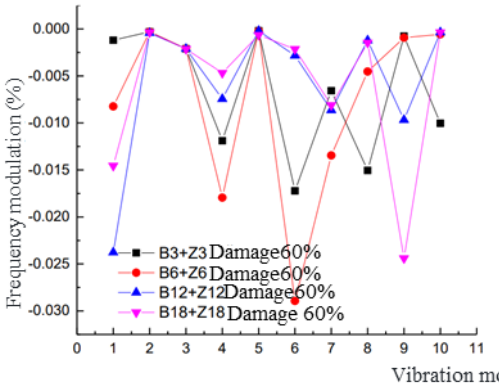

Fig. 24 – The frequency and amplitude variation graph of symmetrical cable damage

The symmetric cable damage on the entire bridge has little effect on the lateral and vertical deflection of the main girder. When symmetrical cable damage occurs on the diagonal cables at 1/3 L~1/2 L of both sides of the main tower, the 6th-order frequency is affected the most, with a frequency variation of up to 2.89%. When symmetrical cable damage occurs on the diagonal cables at 1/2 L~2/3 L of both sides of the main tower, the 1st-order fundamental frequency is affected the most, with a frequency variation of up to 2.38%. Only when the diagonal cables on the inner side of the main tower are symmetrically damaged, the 10th-order frequency is affected.

Dynamic Performance Analysis of Non-symmetric Diagonal Cables with the Same Degree of Damage

For the non-symmetric diagonal cables on both sides of the main tower with the same degree of damage (60%), 12 working conditions are selected for analysis: B3+Z6, B3+Z12, B3+Z18, B6+Z3,

B6+Z12, B6+Z18, B12+Z3, B12+Z6, B12+Z18, B18+Z3, B18+Z6, B18+Z12. The definition of each working condition is shown in Table. 4 - Table. 12. To make a more intuitive comparison of the frequency changes of the non-symmetric diagonal cables under different damage conditions, the 12 damage conditions are merged into 4 working conditions for comparison, as shown in Figure 25 - Figure 28.

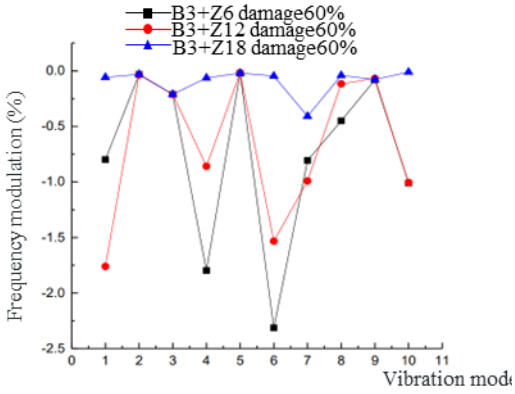

Fig. 25 – Asymmetric cable damage combination condition 1

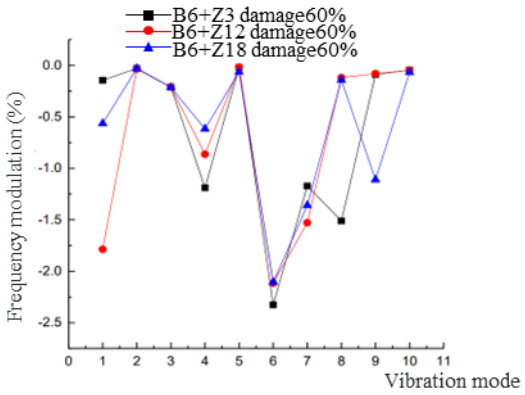

Fig. 26 – Asymmetric cable damage combination condition 2

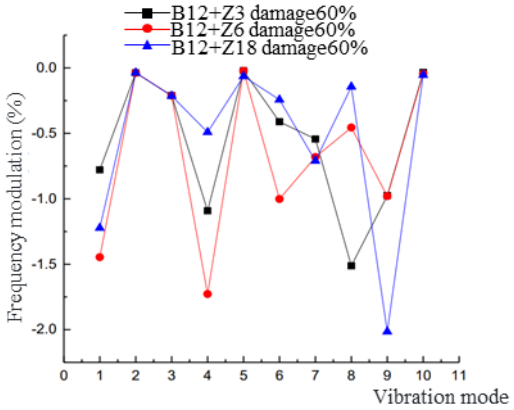

Fig. 27 – Asymmetric cable damage combination condition 3

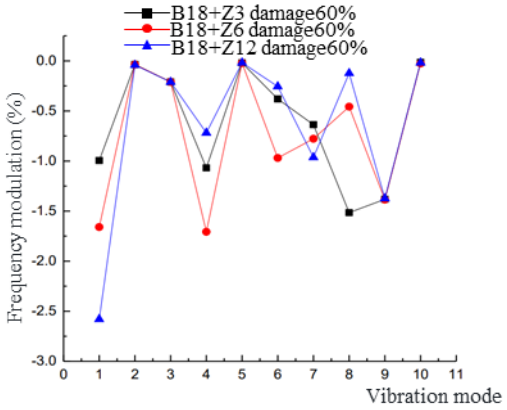

Fig. 28 – Asymmetric cable damage combination condition 4

According to Figure 24, it can be concluded that when there is damage to the inner inclined cable of the auxiliary span and the main span inclined cable is damaged at any position, it will have an impact on the vertical bending of the entire bridge structure. However, it has almost no effect on main beam lateral displacement, main beam vertical displacement, tower column lateral bending, and tower column lateral symmetric bending. Except for the first-order natural frequency of the structure, the farther the damaged position of the main span inclined cable is from the main tower, the smaller the impact on the various natural frequencies of the structure. When there is damage to the inclined cable at 1/3 position of the main span, it has the greatest influence on the sixth-order natural frequency of the structure—main beam first-order symmetric vertical bending, with a maximum change amplitude of 2.31%.

According to Figure 25, it can be concluded that when the inclined cable of the auxiliary span and the short main span at the position of 1/3L~1/2L is damaged, it will have almost no impact on the main beam lateral displacement, tower column lateral bending, and main tower left side main

beam third-order vertical bending, regardless of where the inclined cable of the main span is damaged. When there is damage to the inclined cable at any position of the main tower, the impact on the first and second-order symmetric vertical bending of the main beam on both sides of the main tower is basically the same, with change amplitudes of about 2.30% and 1.50%, respectively. When there is damage to the inner inclined cable of the long main span, it has the greatest influence on the sixth-order natural frequency of the structure—main beam first-order symmetric vertical bending, with a maximum change amplitude of 2.32%.

According to Figure 26, it can be concluded that when the inclined cable of the auxiliary span and the short main span at the position of 1/2L~2/3L is damaged, it will have almost no impact on the main beam lateral displacement, tower column lateral bending, main beam vertical displacement, and main tower left side main beam third-order vertical bending, regardless of where the inclined cable of the main span is damaged. When there is damage to the outer inclined cable of the long main span, it has a significant impact on the ninth-order natural frequency of the structure—tower column lateral symmetric bending, compared to the damage of other inclined cables, with a maximum change amplitude of 2.01%.

Based on Figure 27, it can be concluded that when the inclined cable of the auxiliary span and the outer inclined cable of the short main span is damaged, it will have almost no impact on the main beam lateral displacement, tower column lateral bending, main beam vertical displacement, and main tower left side main beam third-order vertical bending, regardless of where the inclined cable of the main span is damaged. The closer the damaged inclined cable is to the outer side of the main span, the greater the impact on the first-mode vibration of the entire bridge structure, with a maximum change amplitude of 2.58%. When there is damage to any position of the inclined cable of the long main span, the impact on the lower-order frequencies of the entire bridge structure shows a similar trend.

Dynamic Performance Analysis of Pre-stressed π-type Girder Cable-stayed Bridge under Different Cable Damage Conditions

The study aims to investigate the impact of symmetrical damage in different cable locations on the dynamic characteristics of the bridge by selecting four different levels of damage (B3+Z3, B6+Z6, B12+Z12, B18+Z18). The simulation of cable damage is conducted by reducing the elastic modulus of the simulated cable. The dynamic analysis results under different levels of damage for each combination of damaged cables can be seen in Figure 29 - Figure 32.

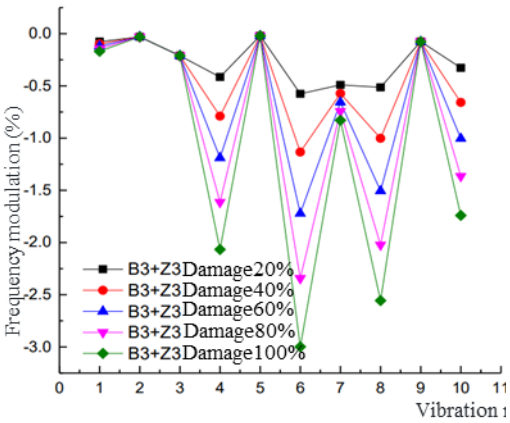

Fig. 29 – Frequency-Amplitude Variation of Symmetrical Cable Damage Condition 1

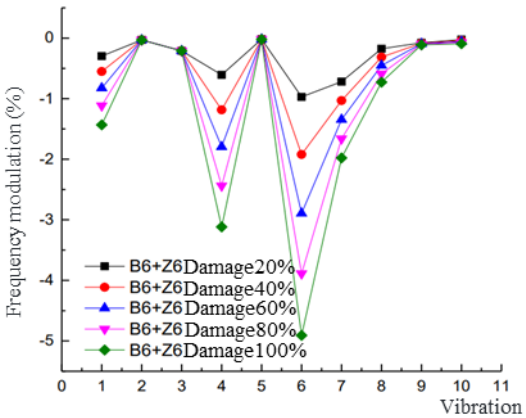

Fig. 30 – Frequency-Amplitude Variation of Symmetrical Cable Damage Condition 2

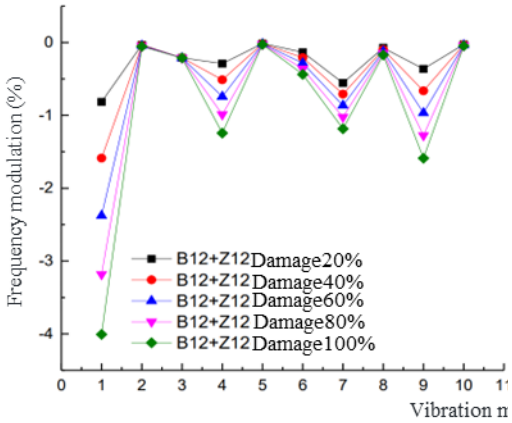

Fig. 31 – Frequency-Amplitude Variation of Symmetrical Cable Damage Condition 3

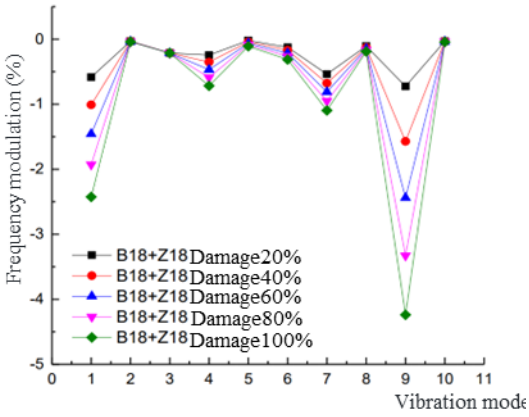

Fig. 32 – Frequency-Amplitude Variation of Symmetrical Cable Damage Condition 4

The symmetric damage in the inner side of the main tower does not significantly affect the first-order natural frequency of the structure, and the frequency-amplitude increases with the increase of damage level. However, it has different impacts on the tenth-order natural frequency of the structure. The impact of symmetric damage of cable-stayed bridge on the dynamic performance is greater than that of damage to a single-side cable or non-symmetric cable; the frequency-amplitude increases by about 2%.

Symmetric damage to cables at various locations will have varying degrees of impact on the vertical bending of the main girder. The effects of symmetric cable damage at different locations are similar to those of non-symmetric and single-side cable damage, and they will not have a significant impact on the lateral deflection of the main girder and the lateral bending of the tower column.

CONCLUSION

1. Damage to the full bridge cables will almost always have varying degrees of impact on the vertical bending of the main girder, but it generally does not affect the lateral and vertical bending modes of the main girder. The varying degree of damage to the cable-stayed bridge has a consistent trend in impacting the dynamic performance of the structure, which is only reflected in the changes in frequency-amplitude. As the level of damage increases, the frequency-amplitude of a certain mode continues to increase.

2. The impact of symmetric damage to cable-stayed bridge on the dynamic performance of the structure is much greater than that of single-side cable damage or non-symmetric damage. Particularly, special attention should be paid to the cases where the outermost cable and the cables located at 1/3L to 1/2L from both sides of the main tower are damaged. When the damage level reaches 100%, the maximum impact on the structural frequency can be around 5%.

REFERENCES

[1] Li H, Ou J. The state of the art in structural health monitoring of cable-stayed bridges[J]. Journal of Civil Structural Health Monitoring, 2016, 6: 43-67.

[2] Martins A M B, Simões L M C, Negrão J H J O. Optimization of cable-stayed bridges: A literature survey[J]. Advances in Engineering Software, 2020, 149: 102829.

[3] Ren W X, Peng X L, Lin Y Q. Experimental and analytical studies on dynamic characteristics of a large span cable-stayed bridge[J]. Engineering Structures, 2005, 27(4): 535-548.

[4] Janjic D, Pircher M, Pircher H. Optimization of cable tensioning in cable-stayed bridges[J]. Journal of bridge engineering, 2003, 8(3): 131-137.
[5] Calvi G M, Sullivan T J, Villani A. Conceptual seismic design of cable-stayed bridges[J]. Journal of Earthquake Engineering, 2010, 14(8): 1139-1171.
[6] Mehrabi A B. In-service evaluation of cable-stayed bridges, overview of available methods and findings[J]. Journal of Bridge Engineering, 2006, 11(6): 716-724.
[7] Wang P H, Tang T Y, Zheng H N. Analysis of cable-stayed bridges during construction by cantilever methods[J]. Computers & Structures, 2004, 82(4-5): 329-346.
[8] Cho S, Yim J, Shin S W, et al. Comparative field study of cable tension measurement for a cable-stayed bridge[J]. Journal of Bridge Engineering, 2013, 18(8): 748-757.
[9] Zhang L, Qiu G, Chen Z. Structural health monitoring methods of cables in cable-stayed bridge: A review[J]. Measurement, 2021, 168: 108343.
[10] Casciati F, Cimellaro G P, Domaneschi M. Seismic reliability of a cable-stayed bridge retrofitted with hysteretic devices[J]. Computers & Structures, 2008, 86(17-18): 1769-1781.
[11] Sung Y C, Chang D W, Teo E H. Optimum post-tensioning cable forces of Mau-Lo Hsi cable-stayed bridge[J]. Engineering Structures, 2006, 28(10): 1407-1417.
[12] Xu Z D, Wu Z. Simulation of the effect of temperature variation on damage detection in a long-span cable-stayed bridge[J]. Structural Health Monitoring, 2007, 6(3): 177-189.
[13] Cao D Q, Song M T, Zhu W D, et al. Modeling and analysis of the in-plane vibration of a complex cable-stayed bridge[J]. Journal of Sound and Vibration, 2012, 331(26): 5685-5714.
[14] Wang H, Tao T, Li A, et al. Structural health monitoring system for Sutong cable-stayed bridge[J]. Smart structures and systems, 2016, 18(2): 317-334.
[15] Tang E K C, Hao H. Numerical simulation of a cable-stayed bridge response to blast loads, Part I: Model development and response calculations[J]. Engineering Structures, 2010, 32(10): 3180-3192.